Surfactant-induced dissipation in sheared foams: mechanics and thermodynamics

Yedhir Mezache, François Detcheverry, Bastien Di Pierro, Peter D M Spelt, Anne-Laure Biance, Marie Le Merrer

Surfactant-induced dissipation in sheared foams: mechanics and thermodynamics.

Yedhir Mezache,[1] François Detcheverry,[1] Bastien Di Pierro,[2] Peter D.M. Spelt,[2,*] Anne-Laure Biance,[1,†] and Marie Le Merrer[1]

[1] *University of Lyon, Université Claude Bernard Lyon 1, CNRS, Institut Lumière Matière, F-69622 Villeurbanne, France.*

[2] *University of Lyon, Université Claude Bernard Lyon 1, Ecole Centrale de Lyon, CNRS, Laboratoire de Mécanique des Fluides et d'Acoustique, F-69622 Villeurbanne, France.*

Though the influence of surfactant type on foam rheological properties is well established experimentally, the underlying physical mechanisms are far from understood. Here, using fully resolved numerical simulation of an elementary T1 event taking into account both flow and surfactant dynamics, we unveil the origin of surfactant-induced dissipation in sheared foams. To model the diffusive and exchange contributions, we revisit the classical Lucassen model by switching from a mechanical to a thermodynamic perspective and find that in spite of its extreme simplicity, it captures well some behaviors of our numerical foam. Our approach should be useful in class of surfactant-controlled systems, from soap films and emulsions to coating films and spreading droplets.

Introduction Foams are soft granular materials made of bubbles in a soapy solution. They are ubiquitous in everyday-life and nature, from shampoos to sea foams and frog nests [1, 2]. Properties such as large specific area, low-cost and low-weight have also made them instrumental in a variety of applications such as cosmetics, fire extinguishers, templates for insulating building materials, or food texture modifiers among others [3]. Understanding the rheology of this class of materials is a long-standing quest [4, 5]. Just as for gels and suspensions, the origin of complex behavior lies in their microstructure. Yet, foams are unique in two aspects. First, the bubbles are soft highly deformable objects, a key property for their organization [6]. Second, these out-of-equilibrium materials involve surface-active species which adsorb at interfaces and induce repulsion forces that stabilize liquid films [7]. These surfactant molecules act as a third component that is essential to the properties of those biphasic systems.

It is now well-established that surfactants play a key role in the rheology of foams [8, 9]. A first line of evidence lies in interfacial rheology, where dedicated models and techniques such as the oscillating bubble method [10, 11] could relate the surfactant mobility in the liquid to the interfacial complex modulus [12, 13], as first proposed by Lucassen [14]. More complex situations include slightly deformed two-bubble assembly or foam [15, 16], or other small deformation modes with viscous dissipation [17, 18]. The effect of the surfactant nature is also apparent in the case of large deformation, such as bubble neighbor switching as evidenced at the bubble scale [19–21] and in 3D foams [22]. The recurring observation is that the type of surfactant, though a component of molecular size, can deeply impact the flow behavior at a much larger scale. Yet, the underlying mechanisms have remained somewhat elusive because experiments typically probe only a global observable such as the loss modulus, and not the "hidden variables" [23] of complex surfactant dynamics.

In this work, we resolve the origin of surfactant-induced dissipation in a flowing foam and its dependency on surfactant properties. Using level-set simulations to probe quantities usually inaccessible in experiments, we present a complete view for the processes at work in the elementary event of a sheared liquid foam. Adopting a thermodynamic point of view, we extended the Lucassen model [14] to propose a tractable prediction for the surfactant-induced dissipation. Though it is a crude representation of a flowing foam, the model is able to rationalize several trends revealed by the simulations. Our approach is applicable to other surfactant-rich systems, from thin films to droplets or bubbly flows.

Dissipation in a numerical sheared foam. The elementary event in a flowing foam is a so-called T1 event, wherein a bubble switches neighbors (Fig. 1a). We consider a minimal two-dimensional system of a few bubbles within a cell of height H (Fig. 1b). Shear is imposed through pinned contact lines by walls moving at a velocity U. The liquid and gas flows are governed by the Navier-Stokes equation for incompressible fluids. The stress-jump boundary condition at the interface involves a Marangoni stress which depends on the surfactant nature and concentration there. The concentrations of surfactants in the liquid and at the interface, F and f resp., evolve through flow advection and through diffusion in the bulk and at the interface with respective coefficient D and D_f. Finally, the exchange of surfactants between the liquid and the interface is described by a Langmuir equation [23], with a flux $J = r_\mathrm{a} F_s(f_\infty - f) - r_\mathrm{d} f$ where r_a and r_d denote the adsorption and desorption rate coefficients, f_∞ is the interfacial concentration at saturation and F_s the subsurface one. All governing equations, definitions of dimensionless quantities and default parameters are detailed in the Supplementary Material (SM [24]).

The surfactant properties are described by three dimensionless numbers: the bulk Péclet number $\mathrm{Pe} \equiv UH/D$, the Biot number $\mathrm{Bi} \equiv r_\mathrm{d} H/U$ and the normalized adsorption length $h \equiv f_\mathrm{e}/F_\mathrm{e} H$, with F_e and f_e the

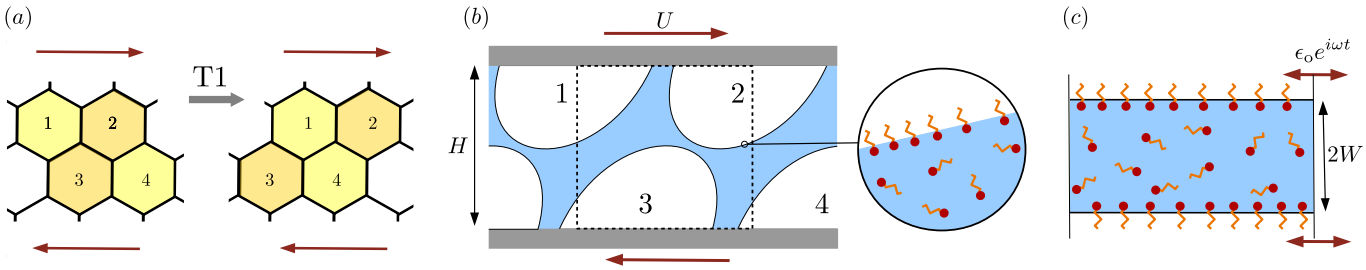

FIG. 1. **Levels of description for dissipation in foams.** (a) A T1 event: upon shearing, bubble 1 and 4 become neighbors. (b) Numerical model of a sheared foam: the 4-bubble assembly sheared by plate motion is solved by the level-set method. The dashed-line rectangle shows the minimal system of interest. (c) Extended Lucassen model: a soap film of thickness $2W$ has its area A subject to sinusoidal relative variations $\epsilon = \delta A/A = \epsilon_0 \exp(i\omega t)$. The model is treated analytically.

values at equilibrium. These parameters may be thought of as characterizing respectively the surfactant diffusion, its sorption dynamics and the relative amount of surfactant lying at the interface with respect to the bulk.

The coupling between liquid flow, surfactant transport, interface boundary condition and the large interface deformation makes for an intricate problem that can only be solved numerically. We use a level-set method [25, 26] extended to account for the surfactant dynamics [27], which allows access to the fluid flow field and local surfactant distribution. Fig. 2 shows a typical view of the various stages of the T1 rearrangement. When the bubble assembly is sheared, the interface may be locally compressed or dilated, inducing enrichment or depletion in surfactants. This induces exchanges with the adjacent liquid resulting in concentration heterogeneities in the bulk, which are counteracted by the smoothing effect of diffusion and possibly by flow advection.

To identify dissipation sources during the T1 process, we use an energy balance. The time-averaged injected power $P_{\rm inj}$ may be evaluated from forces applied on the wall [27]. The average power dissipated by viscosity is $\mathcal{D}_{\rm v} \equiv \langle \mathcal{D}_{\rm v}^{\rm loc} \rangle$, where $\mathcal{D}_{\rm v}^{\rm loc} \equiv \mu \nabla \mathbf{u} : \left(\nabla \mathbf{u} + \nabla \mathbf{u}^{\rm T}\right)$ is the local dissipation due to the gradient of the velocity $\mathbf{u}$, and $\langle \cdot \rangle$ involves both a spatial integration over the whole system and a time average. We observe that $\langle \mathcal{D}_{\rm v} \rangle$ is systematically smaller than $P_{\rm inj}$, with deviations of up to 30%. The difference $\langle \mathcal{D}_{\rm s} \rangle \equiv P_{\rm inj} - \langle \mathcal{D}_{\rm v} \rangle$ is the surfactant-induced dissipation [27], and is the focus of this work.

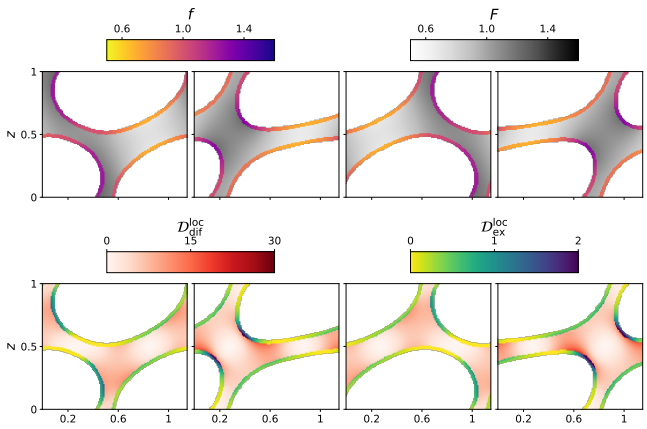

FIG. 2. **Locally resolved T1 event.** Time increases from left to right. Top: surfactant concentration in the liquid and at interface (F and f resp.). Bottom: local rate of dissipation due to surfactant diffusion ($\mathcal{D}_{\rm dif}^{\rm loc}$) and to exchange processes ($\mathcal{D}_{\rm ex}^{\rm loc}$). The simulation parameters are $Pe = 1$, $Bi = 10$ and $h = 1$.

To understand its microscopic origins, we switch from the classical mechanical approach to a thermodynamic framework. According to non-equilibrium thermodynamics [28], the dissipation rate is proportional to the rate of entropy production, where each source contributes through the product of a thermodynamic force and an associated flux. In a sheared foam, the viscous dissipation in the flow is supplemented by two contributions coming from the surfactants. The first is the diffusion contribution, present whenever there are gradients in surfactant concentration [29]; the second is the exchange contribution deriving from adsorption/desorption processes at the interface. Their local dissipation rates, per unit volume and unit interfacial area respectively, are (SM [24]):

$$\mathcal{D}_{\rm dif}^{\rm loc} = \nabla \mu_F (D \nabla F) = DRT(\nabla F)^2/F, \qquad (1a)$$

$$\mathcal{D}_{\rm ex}^{\rm loc} = J(\mu_{F_s} - \mu_f) \simeq RTJ^2/(r_{\rm d} f_{\rm e}), \qquad (1b)$$

with R the ideal gaz constant and T the temperature. In Eq. (1a), the last equality assumes that the chemical potential of the surfactants in the liquid is $\mu_F = \mu_0 + RT \ln F/F_{\rm e}$. In Eq. (1b), the thermodynamic force is the difference of chemical potentials between the surface ($\mu_f = \mu_0 + RT \ln[f/(f_\infty - f)]$) and the adjacent liquid ($\mu_{F_s} = \mu_F(F = F_s)$). The last equality is valid close to equilibrium.

We first check the consistency of our description. Besides its definition as $\langle \mathcal{D}_{\rm s} \rangle \equiv P_{\rm inj} - \langle \mathcal{D}_{\rm v} \rangle$, $\langle \mathcal{D}_{\rm s} \rangle$ can also be expressed thermodynamically as $\langle \mathcal{D}_{\rm dif}^{\rm loc} \rangle + \langle \mathcal{D}_{\rm ex}^{\rm loc} \rangle$. A third alternative formulation from purely mechanical considerations [27] is $\langle \int_\Gamma \gamma \nabla_{\rm s} \cdot \mathbf{u} \, d\Gamma \rangle$, with Γ the interface contour, γ the surface tension and ∇_s the surface divergence. We find (SM [24]) that the three numerical estimates for $\langle \mathcal{D}_{\rm s} \rangle$ match each other, typically within 10% due to discretiz-

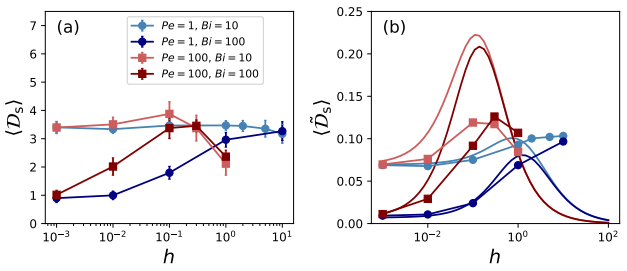

FIG. 3. **Dependence of surfactant dissipation on surfactant properties** (a) Simulation: surfactant dissipation $\langle \mathcal{D}_\mathrm{s} \rangle$ as a function of h for various Pe and Bi. (b) Rescaled surfactant dissipation $\langle \tilde{\mathcal{D}}_\mathrm{s} \rangle$ in the Lucassen model (thick lines) and in simulations (points).

ing errors reflected in the errorbars of Fig. 3a. This approximate agreement confirms that no important source of surfactant dissipation has been left out.

As expected, the surfactant properties do significantly influence the dissipation. The total surfactant dissipation is shown in Fig. 3 for various combinations of Pe, Bi and h, which characterize the surfactant nature. We observe a highly non-trivial behaviour, with a maximum dissipation that appears at intermediate values of h. The rationale for this behavior is difficult to pinpoint at this stage.

Whether surfactant dissipation is dominated by diffusion or exchange processes depends on the surfactant properties. The ratio $\langle \mathcal{D}_\mathrm{dif} \rangle / \langle \mathcal{D}_\mathrm{ex} \rangle$ obtained numerically for a variety of Pe, Bi and h values varies by several orders of magnitude (Fig. 4a). Is the difference reflected in the maps of surfactant distribution and dissipation? Consider first the exchange dominated regime, as in case 1 of Fig. 4. Here, the surfactant distribution is very homogeneous both in the bulk and at the interface. Consequently, dissipation due to diffusion across the liquid bulk is weak compared to dissipation generated by surfactant exchanges with the interface. The situation is reversed upon increasing Péclet to Pe = 100, i.e. taking a surfactant with much lower diffusivity (case 2 of Fig. 4). The diffusion contribution becomes dominant because the surfactants in the bulk and at the interface are heterogeneously distributed. Dissipation due to diffusion is then more pronounced and localized in the vicinity of the interfaces. Finally , a different dissipation pattern can be observed by varying h while keeping the same ratio $\langle \mathcal{D}_\mathrm{dif} \rangle / \langle \mathcal{D}_\mathrm{ex} \rangle$ (case 3 of Fig. 4). Here the concentration and dissipation heterogeneities are parallel to the interface, instead of being normal as in case 2. Overall, we observe that how and where dissipation occurs depends sensitively on surfactant properties.

Extended Lucassen model. To shed light on these numerical observations, we revisit the 60-year old model of Lucassen and van den Tempel [14] who first rationalized how surfactant dynamics could induce an effective surface viscosity [30]. For the simplified geometry of Fig. 1c, we study how a liquid film of finite thickness $2W$ that contains surfactants responds to an imposed area variation of relative amplitude ϵ_0 and pulsation ω. Our approach differs from the original model in two ways: *(i)* Instead of instantaneous exchanges and an infinite reservoir, we assume both a finite adsorption/desorption kinetics and a finite thickness for the film. Though these extensions were considered separately [13, 31], we treat the general case here. *(ii)* More importantly, we adopt a complementary thermodynamic view where we compute not only the loss modulus that encapsulates all dissipative relaxation processes, but also the separate contributions from each dissipation mechanism, allowing a measure of their relative importance. The calculations for this extended Lucassen model are fully detailed in SM [24].

The main result is a set of explicit formulas for dissipation induced by diffusion and sorption of surfactants. To quote the result, we introduce the dimensionless numbers $\mathrm{Pe} \equiv \omega W^2/D$, $\mathrm{Bi} \equiv r_\mathrm{d}/\omega$ and $h = f_\mathrm{e}/F_\mathrm{e} W$, whose definitions match those used for the simulations with the substitution $H = W$ and $U = \omega W$. Focusing on time and spatial average for simplicity, we find that:

$$\frac{\langle \mathcal{D}_\mathrm{dif} \rangle}{\mathcal{D}_\mathrm{un}} = \frac{\bar{\chi} h \sqrt{8\mathrm{Pe}}}{\left| \zeta^{-1} + 1 - i \right|^2} \mathcal{G}(\sqrt{2\mathrm{Pe}}), \tag{2a}$$

$$\frac{\langle \mathcal{D}_\mathrm{ex} \rangle}{\mathcal{D}_\mathrm{un}} = \frac{4\bar{\chi}}{\mathrm{Bi} |\zeta^{-1} + 1 - i|^2}, \tag{2b}$$

$$\text{with } \frac{\zeta^{-1}}{\sqrt{2}\bar{\chi}} \equiv h\sqrt{\mathrm{Pe}} \coth\left(j\sqrt{\mathrm{Pe}}\right) + \frac{j}{\mathrm{Bi}}, \quad j \equiv \frac{1+i}{\sqrt{2}}$$

with $\mathcal{G}(u) \equiv (\sinh u - \sin u)/(\cosh u - \cos u)$, and $1 - \bar{\chi} \equiv \chi \equiv f_\mathrm{e}/f_\infty$ a parameter for surface coverage that remains constant. The left-hand sides are made dimensionless with $\mathcal{D}_\mathrm{un} \equiv E_\mathrm{GM} \omega \epsilon_0^2/2$, where E_GM is the Gibbs-Marangoni elasticity modulus [12]. Thus, from the physico-chemical properties of the surfactants as specified through the dimensionless numbers, Eqs. (2a) and (2b) can predict the origins and magnitudes of surfactant dissipation induced by solicitation of the interface.

As a first application, we consider the total surfactant-induced dissipation $\langle \mathcal{D}_\mathrm{s} \rangle \equiv \langle \mathcal{D}_\mathrm{dif} \rangle + \langle \mathcal{D}_\mathrm{ex} \rangle$ in our extended Lucassen model (Fig. 3b). For $h \to 0$ a plateau is reached, whose value $\bar{\chi}\mathrm{Bi}/(\bar{\chi}^2 + \mathrm{Bi}^2)$ is independent of Pe. For $h \to \infty$, $\langle \mathcal{D}_\mathrm{s} \rangle$ decreases as h^{-1}. At intermediate values of h, $\langle \mathcal{D}_\mathrm{s} \rangle$ exhibits a maximum, whose location and value can be expressed analytically in the limit of high Bi that is relevant here (SM [24]). For instance, $h_\mathrm{max} \simeq 1/\bar{\chi}\sqrt{\mathrm{Pe}}$ in the limit of large Pe. The maximum defines a characteristic length scale $f_\mathrm{e}/F_\mathrm{e} h_\mathrm{max}$ that when matching the system size H results in exacerbated surfactant dissipation. For large values of h, the surfactant dissipation always vanishes.

To compare the surfactant dissipation in the model and in simulations, the use of a re-scaled dissipation $\langle \tilde{\mathcal{D}}_\mathrm{s} \rangle$ is required. For the model, $\langle \tilde{\mathcal{D}}_\mathrm{s} \rangle \equiv \langle \mathcal{D}_\mathrm{s} \rangle / \mathcal{D}_\mathrm{un}$. For the

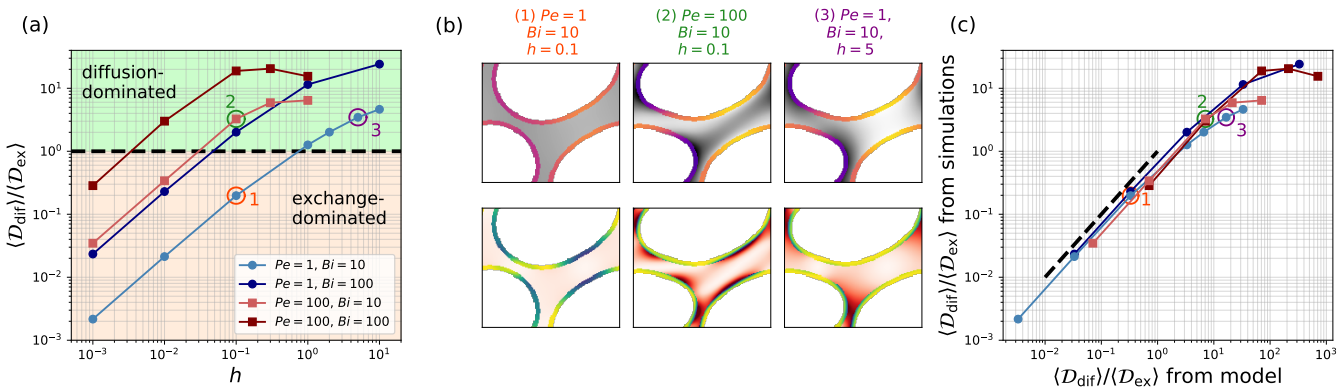

FIG. 4. **Origin of surfactant dissipation.** (a) Ratio $\langle \mathcal{D}_{\rm dif} \rangle / \langle \mathcal{D}_{\rm ex} \rangle$ as a function of h for various Pe and Bi, as obtained from simulations. (b) Maps of local concentration (top) and dissipation (bottom) for cases 1-2 and 3 circled in (a) and (c). The color scales are the same as in Fig. 2. (c) Ratio $\langle \mathcal{D}_{\rm dif} \rangle / \langle \mathcal{D}_{\rm ex} \rangle$: The simulation data is plotted as a function of the extended Lucassen prediction (Eq. 3). The dashed black line shows the identity function.

simulations, $\langle \tilde{\mathcal{D}}_{\rm s} \rangle \equiv \xi \langle \mathcal{D}_{\rm s} \rangle / \mathcal{C}$, where ξ is a constant [32], and $\mathcal{C} \equiv \langle \int_\Gamma (\nabla_s \cdot \mathbf{u})^2 d\Gamma \rangle$ accounts for a heterogeneous dilatation along the interface. The rescaled dissipations $\langle \tilde{\mathcal{D}}_{\rm s} \rangle$ for model and simulation show common features (Fig. 3b). The Pe-independent plateaus at low h match quantitatively, whereas the existence and location of the maximum agrees at least qualitatively. We ascribe the deviation at large h to longitudinal concentration gradients which exist in simulations (see Fig. 4b) but are neglected in the one-dimensional geometry of our model.

As a second comparison, we now identify which mechanism dominates the surfactant dissipation. In this regard, the prediction of the extended Lucassen model is remarkably simple:

$$\frac{\langle \mathcal{D}_{\rm dif} \rangle}{\langle \mathcal{D}_{\rm ex} \rangle} = \mathrm{Da}\ \mathcal{G}(\sqrt{2\mathrm{Pe}}), \tag{3}$$

with $\mathcal{G}$ defined after Eq. (2b), and $\mathrm{Da} = \bar{\chi}\, h\, \mathrm{Bi} \sqrt{\mathrm{Pe}/2}$ the Damköhler number, which compares sorption and diffusion timescales. Plotting the simulation data for $\langle \mathcal{D}_{\rm dif} \rangle / \langle \mathcal{D}_{\rm ex} \rangle$ versus the model prediction (Fig. 4c), we observe a good collapse of all the curves, whatever the parameters considered. Moreover, for all low or intermediate h values, the data and prediction are proportional to each other (with a prefactor ≈ 0.6), showing the ability of the simple model to capture a complex system. To explain the deviations visible at large h, we recall that the model assumes lateral invariance of surfactant concentration, which has two consequences. First, the contribution from surfactant diffusion along the interface is neglected. This is actually legitimate since this term is numerically negligible [33]. Second, concentration gradients parallel to the interface are forbidden. This is different from simulations (cases 2-3 Fig. 4), pointing to a possible cause for discrepancy at large ratios values. Overall, although its geometry is drastically simplified compared to a sheared foam, the model is able to capture some of the generic features of the dissipation mechanisms.

Conclusion To summarize, we investigated numerically the surfactant dissipation in a sheared foam and found that an extended Lucassen model is sufficient to rationalize some key features. In both simulations and in a simplified model, we used a thermodynamic approach to identify which transport mechanisms – diffusion or exchange – dominates surface dissipation. Our findings may help to rationalize the influence of surfactants on foam behavior. Strong effects of surfactant physicochemistry are reported [8, 20–22], when insoluble surfactants (e.g. dodecanol, fatty acids) are added to solutions of soluble ones (e.g. sodium dodecyl sulfate, SLES-CAPB mixtures). In terms of dimensionless numbers, the insoluble and soluble molecules are similar in size, hence in Pe numbers, and the adsorption lengths vary from 1 to 5 μm [18], leading to h values with comparable order of magnitude. By contrast, exchanges can be slowed down by three orders of magnitude in the presence of insoluble species [34], corresponding to a decrease in Biot number by a factor 10^3. Our results (Fig. 3) show that lowering Bi can increase the total surface dissipation. Such a trend is qualitatively consistent with the observed increase of foam viscosity [8] and slowing down of bubble rearrangements [20–22], and suggests that surfactant dissipation might be one key factor controlling the impact of surfactant composition on foam rheology.

This work should be pursued in several directions. First, it motivates further experimental work aimed at correlating specific microscopic surfactant properties and rheological measurements. Second, future efforts must be made towards extending our model to account for the viscous dissipation in the fluid, so as to better understand its coupling with surfactant properties and overall foam rheology. Finally, from a wider perspective, the methodology presented here is not specific to foams but is applicable to many surfactant-controlled systems, in-

cluding emulsions [9], drop and bubble dynamics [35] and thin films [36].

Acknowledgements This research was funded by a grant from ANR (project Surfbreak, ANR-18-CE08-0013, 2018). We thank Isabelle Cantat and Christophe Ybert for inspiring discussions.

* Deceased 2020
† anne-laure.biance@univ-lyon1.fr

[1] Cantat, I., Cohen-Addad, S., Elias, F., Graner, F., Hohler, R., Pitois, O., Rouyer, F., Saint-James, A., *Foams - Structure and Dynamics*, (Oxford 2013).
[2] Hill, C., Eastoe, J., Foams: From nature to industry. *Adv. Colloid Interface Sci.* **247**, 469 (2017).
[3] Stevenson, P., *Foam engineering: fundamentals and applications*, (John Wiley & Sons 2012).
[4] Weitz, D., Foam flow by stick and slip. *Nature* **381**, 475 (1996).
[5] Höhler, R., Cohen-Addad, S., Rheology of liquid foam. *J. Phys.: Condens. Matter* **17**, R1041 (2005).
[6] Drenckhan, W., Hutzler, S., Structure and energy of liquid foams. *Advances in colloid and interface science* **224**, 1 (2015).
[7] Bergeron, V., Forces and structure in thin liquid soap films. *J. Phys.: Condens. Matter* **11**, R215 (1999).
[8] Denkov, N. D., Tcholakova, S., Golemanov, K., Ananthpadmanabhan, K. P., Lips, A., The role of surfactant type and bubble surface mobility in foam rheology. *Soft Matter* **5**, 3389 (2009).
[9] Cohen-Addad, S., Höhler, R., Pitois, O., Flow in Foams and Flowing Foams. *Annu. Rev. Fluid Mech.* **45**, 241 (2013).
[10] Johnson, D. O., Stebe, K. J., Oscillating bubble tensiometry: A method for measuring the surfactant adsorptive-desorptive kinetics and the surface dilatational viscosity. *J. Colloid Interface Sci.* **168**, 21 (1994).
[11] Wantke, K.-D., Fruhner, H., in *Studies in Interface Science*.
[12] Langevin, D., Rheology of Adsorbed Surfactant Monolayers at Fluid Surfaces. *Annu. Rev. Fluid Mech.* **46**, 47 (2014).
[13] Christov, C., Ting, L., Wasan, D., The apparent dilational viscoelastic properties of fluid interfaces. *J. Colloid Interface Sci.* **85**, 363 (1982).
[14] Lucassen, J., Van Den Tempel, M., Dynamic measurements of dilational properties of a liquid interface. *Chem. Eng. Sci.* **27**, 1283 (1972).
[15] Besson, S., Debrégeas, G., Statics and dynamics of adhesion between two soap bubbles. *Eur. Phys. J. E* **24**, 109 (2007).
[16] Besson, S., Debrégeas, G., Cohen-Addad, S., Höhler, R., Dissipation in a sheared foam: From bubble adhesion to foam rheology. *Phys. Rev. Lett.* **101**, 214504 (2008).
[17] Bussonnière, A., Shabalina, E., Ah-Thon, X., Le Fur, M., Cantat, I., Dynamical Coupling between Connected Foam Films: Interface Transfer across the Menisci. *Phys. Rev. Lett.* **124**, 018001 (2020).
[18] Bussonnière, A., Cantat, I., Local origin of the viscoelasticity of a millimetric elementary foam. *J. Fluid Mech.* **922**, A25 (2021).
[19] Durand, M., Stone, H. A., Relaxation Time of the Topological T1 Process in a Two-Dimensional Foam. *Phys. Rev. Lett.* **97**, 226101 (2006).
[20] Biance, A., Cohen-Addad, S., Höhler, R., Topological transition dynamics in a strained bubble cluster. *Soft Matter* **5**, 4672 (2009).
[21] Petit, P., Seiwert, J., Cantat, I., Biance, A., On the generation of a foam film during a topological rearrangement. *J. Fluid Mech.* **763**, 286 (2015).
[22] Le Merrer, M., Cohen-Addad, S., Höhler, R., Duration of bubble rearrangements in a coarsening foam probed by time-resolved diffusing-wave spectroscopy: Impact of interfacial rigidity. *Phys. Rev. E* **88**, 022303 (2013).
[23] Manikantan, H., Squires, T. M., Surfactant dynamics: Hidden variables controlling fluid flows. *J. Fluid Mech.* **892**, 1 (2020).
[24] Supplementary material is available at...
[25] Osher, S., Fedkiw, R., *Level Set Methods and Dynamic Implicit Surfaces*, volume 153, (Springer 2003).
[26] Sethian, J. A., Smereka, P., Level set methods for fluid interfaces. *Annu. Rev. Fluid Mech.* **35**, 341 (2003).
[27] Titta, A., Le Merrer, M., Detcheverry, F., Spelt, P., Biance, A.-L., Level-set simulations of a 2D topological rearrangement in a bubble assembly: effects of surfactant properties. *J. Fluid Mech.* **838**, 222 (2018).
[28] de Groot, S. R., Mazur, P., *Non-Equilibrium Thermodynamics*, (Dover, New York 1984).
[29] Buzza, D. M. A., Lu, C. Y. D., Cates, M. E., Linear Shear Rheology of Incompressible Foams. *Journal De Physique II* **5**, 37 (1995).
[30] Levich, V. G., *Physicochemical Hydrodynamics*, (Prentice-Hall, Englewood Cliffs 1962).
[31] van den Tempel, M., Lucassen, J., Lucassen-Reynders, E. H., Application of surface thermodynamics to Gibbs elasticity. *J. Phys. Chem.* **69**, 1798 (1965).
[32] Specifically, $\xi \equiv \mathrm{Re}Ca_0\bar{\chi}/\beta\chi$, where the Reynolds number Re, capillary number Ca_0 and β parameters are defined in SM [24].
[33] Because of the high surface Péclet number $\mathrm{Pe}_f \equiv HU/D_f = 10^3$, this term contributes to less than 2% of the total dissipation in 21 out of 22 simulations. The only exception is 10% when $\mathrm{Pe} = 100$, $\mathrm{Bi} = 10$, $h = 1$.
[34] Minkov, I. L., Arabadzhieva, D., Salama, I. E., Mileva, E., Slavchov, R. I., Barrier kinetics of adsorption–desorption of alcohol monolayers on water under constant surface tension. *Soft matter* **15**, 1730 (2019).
[35] Anna, S. L., Droplets and bubbles in microfluidic devices. *Annual Review of Fluid Mechanics* **48**, 285 (2016).
[36] Ou Ramdane, O., Quéré, D., Thickening factor in marangoni coating. *Langmuir* **13**, 2911 (1997).